

Long-Term Evolution of Massive Black Hole Binaries. II. Binary Evolution in Low-Density Galaxies

Peter Berczik^{1,2,3}, David Merritt² and Rainer Spurzem³

ABSTRACT

We use direct-summation N -body integrations to follow the evolution of binary black holes at the centers of galaxy models with large, constant-density cores. Particle numbers as large as 0.4×10^6 are considered. The results are compared with the predictions of loss-cone theory, under the assumption that the supply of stars to the binary is limited by the rate at which they can be scattered into the binary's influence sphere by gravitational encounters. The agreement between theory and simulation is quite good; in particular, we are able to quantitatively explain the observed dependence of binary hardening rate on N . We do not verify the recent claim of Chatterjee, Hernquist & Loeb (2003) that the hardening rate of the binary stabilizes when N exceeds a particular value, or that Brownian wandering of the binary has a significant effect on its evolution. When scaled to real galaxies, our results suggest that massive black hole binaries in gas-poor nuclei would be unlikely to reach gravitational-wave coalescence in a Hubble time.

Subject headings: black hole physics — galaxies: nuclei — stellar dynamics

1. Introduction

Binary supermassive black holes are inevitable by-products of galaxy mergers, and their coalescence is potentially the strongest source of gravitational waves in the universe (Thorne & Braginskii 1976). Following their initial formation at separations of roughly a parsec, massive binaries are expected to “harden” as the two black holes exchange angular momentum with stars or gas in the host galaxy's nucleus. The binary separation must decrease by 1-2 orders of magnitude if the black holes are to come close enough together that gravitational wave emission can induce coalescence in a Hubble time. Whether this happens in most galaxies, or whether uncoalesced binaries are the norm, is currently an unanswered question (Merritt & Milosavljevic 2004).

This paper is the second in a series investigat-

ing the long-term evolution of binary black holes in galactic nuclei. As in Paper I (Milosavljević & Merritt 2003), we restrict our attention to galaxies without gas. In such an environment, a massive binary shrinks as passing stars extract energy and angular momentum from it via the gravitational slingshot (Saslaw et al. 1974). Early treatments of binary evolution (Baranov 1984; Mikkola & Valtonen 1992; Rajagopal & Romani 1995; Quinlan 1996) represented the galaxy as fixed in its properties as the binary evolved, and inferred the binary's evolution from rate coefficients derived via three-body scattering experiments. This approximation is reasonable during the binary's initial evolution, but once the separation has decreased by a factor of order unity, the assumption of a fixed background is no longer valid. The binary quickly (in a galaxy crossing time) interacts with and ejects most of the stars on intersecting orbits, and any subsequent binary-star interactions require a repopulation of the orbits in the binary's “loss cone.” This argument has motivated various hybrid approaches to binary evolution, in which a model for loss-cone repopulation is coupled with rate coefficients derived from scattering experi-

¹Main Astronomical Observatory, National Academy of Sciences of Ukraine, Kiev, Ukraine

²Department of Physics, Rochester Institute of Technology, Rochester, NY

³Astronomisches Rechen-Institut, Zentrum für Astronomie, Universität Heidelberg, Heidelberg, Germany

ments in a fixed background (Zier & Biermann 2001; Yu 2002; Milosavljević & Merritt 2003; Merritt & Poon 2004; Merritt & Wang 2005).

Two regimes of loss-cone repopulation can be identified (Paper I). If the time scale for encounters (or some other process) to drive stars into the binary is short compared with orbital periods, the binary’s loss cone will remain nearly “full,” and the rate of supply of stars will hardly be affected by their loss due to ejections. On the other hand, if time scales for loss-cone repopulation are long compared with orbital periods, the binary’s loss cone will be nearly “empty,” and the binary’s evolution will be limited by the rate at which new stars can diffuse onto loss-cone orbits. If the diffusion is driven by star-star gravitational encounters, the binary’s hardening rate in this regime will scale approximately as N^{-1} (in a galaxy with fixed mass and radius). For values of N characteristic of real galaxies, $N \gtrsim 10^{10}$, encounters would be rare enough that the loss cone of a massive binary would remain nearly empty, and the hardening rate would correspondingly be very low. In effect, the decay would stall.

While the hybrid models are informative, a fully self-consistent, N -body approach to the evolution of massive binaries is clearly desirable. Scattering experiments in a homogeneous background do not faithfully reproduce the interactions that take place at the bottom of a galactic potential well, where a given star may interact more than once with the binary (Kandrup et al. 2003; Milosavljević & Merritt 2003). If the goal is to follow the evolution starting from the pre-merger phase, when the two black holes were widely separated, N -body techniques are unavoidable. However most N -body simulations of binary evolution published to date (Ebisuzaki et al. 1991; Makino et al. 1993; Governato et al. 1994; Milosavljević & Merritt 2001) have been based on such small particle numbers that the binary’s loss cone was kept essentially full by star-star scattering or by random motion of the binary. As a consequence, these simulations failed to reproduce the diffusive loss cone repopulation that would characterize binary evolution in the large- N limit and they can not easily be scaled to real galaxies.

In this paper, we consider the N -body evolution of a massive binary in a very idealized galaxy model, with a Plummer (1911) density profile.

The Plummer model has a large, constant-density core, rather different from the power-law nuclei of most galaxies. There are several reasons for this unphysical choice. (1) The low central concentration of the Plummer model implies a long star-star relaxation time, hence our N -body models are able to maintain an empty loss cone with fewer particles than would be required if we had used a more realistic galaxy model. This allows us to approach more closely than heretofore to the diffusive loss-cone repopulation regime. (2) Also because of its low central concentration, the Plummer model evolves only slightly due to the influence of the binary. This makes it easier to compare our N -body results with a model in which the gross properties of the galaxy are assumed to remain fixed with time. (3) Our initial conditions are precisely the same as those adopted by Chatterjee, Hernquist & Loeb (2003) in their numerical study of binary evolution. These authors used a hybrid N -body code in order to achieve large particle numbers and reached a striking, counter-intuitive conclusion about the N -dependence of the binary hardening rate. Based on this result, Chatterjee et al. concluded that “a substantial fraction of all massive binaries in galaxies can coalesce within a Hubble time.” As discussed below, we fail to confirm their result with our higher-accuracy integrations, and reach a different conclusion about the likelihood of coalescence.

The N -body integrations presented here were the first to be carried out on a new, special-purpose computer that couples GRAPE hardware with a parallel architecture. §2 describes the computer, the N -body algorithm and the tests which we carried out to verify its accuracy. The evolution of the binary is described in §3, and in §4 we show how the N -body evolution can be reconciled with the predictions of collisional loss-cone theory. Our results are compared with those of earlier studies in §5, and §6 briefly discusses some implications of our results for binary evolution in real galaxies. §7 sums up.

2. Models and Methods

Our initial galaxy model was a Plummer (1911) sphere, with mass density and gravitational poten-

tial given by

$$\rho(r) = \frac{3}{4\pi} \frac{M_{gal}}{r_0^3} (1+x^2)^{-5/2}, \quad (1a)$$

$$\Psi(r) = GM_{gal} (1+x^2)^{-1/2}, x \equiv r/r_0. (1b)$$

Here M_{gal} is the total galaxy mass, r_0 is the Plummer scale length and G is the gravitational constant. We henceforth adopt standard N -body units (Heggie & Mathieu 1986), $G = M_{gal} = 1$, $E = 1/4$ with E the total (binding) energy; in these units, $r_0 = 3\pi/16 \approx 0.589$. Particle positions and velocities were generated in the usual way from the equilibrium, energy-dependent distribution function $f(E)$.

Our galaxy model was the same one adopted by Chatterjee et al. (2003) in their N -body study of binary evolution. We also followed their prescription for introducing the massive binary into the galaxy: two point masses of equal mass, $M_1 = M_2 = M/2$, were placed on nearly circular orbits at \mathbf{r} and $-\mathbf{r}$, with $r = 0.3$. No adjustments were made in the stellar positions and velocities when introducing the black hole particles. We chose two values for the masses of the black holes: $M_1 = M_2 = 0.02$ and $M_1 = M_2 = 0.005$. Integrations were continued until a time of $t = 250$, corresponding to roughly 88 crossing times, where $T_{cr} \equiv (2|E|)^{-3/2} \approx 2.83$. We carried out integrations with a range of particle numbers, $N = (0.05, 0.1, 0.2, 0.4) \times 10^6$, in order to test the dependence of the results on N .

The sphere of influence of a (single) black hole of mass M is $r_h \equiv GM/\sigma(0)^2$ with $\sigma(0)$ the 1D stellar velocity dispersion at the center of the galaxy. In our Plummer spheres, $\sigma(0) = (2/3)\sqrt{2/\pi} \approx 0.532$, yielding $r_h = (0.141, 0.0353)$ for $M = M_1 + M_2 = (0.04, 0.01)$. The semimajor axis at which a binary first becomes ‘‘hard’’ is given approximately by $a_h = GM_2/4\sigma^2$ with M_2 the mass of the small component (Quinlan 1996); for an equal-mass binary, $a_h = r_h/8 = (1.76 \times 10^{-2}, 4.42 \times 10^{-3})$ for $M = (0.04, 0.01)$. Thus, the two black hole particles moved initially on widely separated, nearly independent orbits.

The N -body integrations were carried out on gravitySimulator,¹ a special-purpose computer cluster recently installed at the Rochester Insti-

tute of Technology. This cluster contains 32 dual-Xeon nodes running at 3.0 GHz. Each node hosts a single GRAPE-6A accelerator board (Fukushige et al. 2005) which can store data for up to 131,072 particles and calculate at a speed of 125 GFlops, allowing the entire cluster to carry out simulations with particle numbers of $\sim 4 \times 10^6$ and at speeds of approximately 4 TFlops. Communication between the GRAPE boards and their host nodes is via the standard PCI (32bit/33MHz) interface; the PC nodes are connected via a high-speed Infiniband network switch with bandwidth of 10 Gbit/s (duplex).

The N -body code was an adaptation of Aarseth’s NBODY1 (Aarseth 1999) to the GRAPE cluster. The gravitational force acting on particle i is

$$\mathbf{F}_i = m_i \mathbf{a}_i = -m_i \sum_{k=1, k \neq i}^N \frac{m_k (\mathbf{r}_i - \mathbf{r}_k)}{(\epsilon^2 + |\mathbf{r}_i - \mathbf{r}_k|^2)^{3/2}} \quad (2)$$

where m_i and \mathbf{r}_i are the mass and position of the i th particle and ϵ is the softening length; the gravitational force constant has been set to one. The integration of particle orbits was based on the fourth-order Hermite scheme as described by Makino and Aarseth (1992). We adopted their formula for computing the time-step of an individual particle i at time t ,

$$\Delta t_i = \sqrt{\eta \frac{|\mathbf{a}(t)| |\mathbf{a}^{(2)}(t)| + |\dot{\mathbf{a}}(t)|^2}{|\dot{\mathbf{a}}(t)| |\mathbf{a}^{(3)}(t)| + |\mathbf{a}^{(2)}(t)|^2}}. \quad (3)$$

Here \mathbf{a} is the acceleration of the i th particle, the superscript (j) denotes the j ’th time derivative, and η is a dimensionless constant that sets the accuracy of the integrator. Since the particle positions \mathbf{r}_k must be up-to-date in equation (2) they are predicted using a low order polynomial. This prediction takes less time if groups of particles request a new force calculation at large time intervals, rather than if single particles request it in small time intervals. For this reason, an integer n is chosen such that

$$\left(\frac{1}{2}\right)^n \leq \Delta t_i < \left(\frac{1}{2}\right)^{n-1} \quad (4)$$

with Δt_i given by equation (3). The individual time step is replaced by a block time step $\Delta_b t_i$, where

$$\Delta_b t_i = \left(\frac{1}{2}\right)^n. \quad (5)$$

¹<http://www.cs.rit.edu/~grapecluster/>

The parallel algorithm begins by distributing the N particles randomly and evenly between the p GRAPEs. At each time step, the active particles on each node (i.e. the particles whose positions are due for an update) are identified and their coordinates broadcast to all of the other nodes, where the partial forces are computed. The partial forces are summed on the head node where the positions and velocities of the active particles are advanced, and their coordinates are then updated in the individual GRAPE memories. More details of the parallel algorithm, including the results of extensive performance tests, are given in an upcoming paper (Harfst et al. 2005). Most of the integrations used eight nodes; integrations with the largest particle numbers ($N = 0.4 \times 10^6$) used either 16 or 32 nodes.

The N -body code has two important parameters that affect the accuracy and efficiency of the integrations: the softening length ϵ and the time step parameter η . Figure 1 shows the effects of varying ϵ and η on the evolution of a binary with mass $M_1 = M_2 = 0.02$ in a Plummer-model galaxy with $N = 0.05 \times 10^6$. The initial positions and velocities of the two massive particles were the same as in the “production” runs. The overall accuracy of the calculation as measured by changes in energy $|\Delta E/E|$ (Fig. 1(a)) depends most strongly on the time-step parameter η ; for $\eta = 0.01$, the fractional change in E is a few percent or less. Figure 1(b) shows that most of the error in the total energy comes from the binary, which is very poorly integrated when η is as large as 0.03. This figure suggests that a value $\eta = 0.02$ or smaller is required for accurate long-term integration of the binary. The evolution of the binary’s eccentricity (Fig. 1(c)) is also poorly reproduced when $\eta = 0.03$. Changing the softening length ϵ appears to have much less effect on the evolution of a or e , although of course ϵ must be small compared with the smallest separation attained by the binary. Based on these tests, we adopted $\eta = 0.01$ and $\epsilon = 1 \times 10^{-4}$ for the final integrations.

3. Evolution of the Binary

Figure 2 shows the evolution of the binary’s semi-major axis in each of the eight integrations. The N -dependence of the hardening rate is clear. At late times, when $a \ll a_h$, the binary semi-

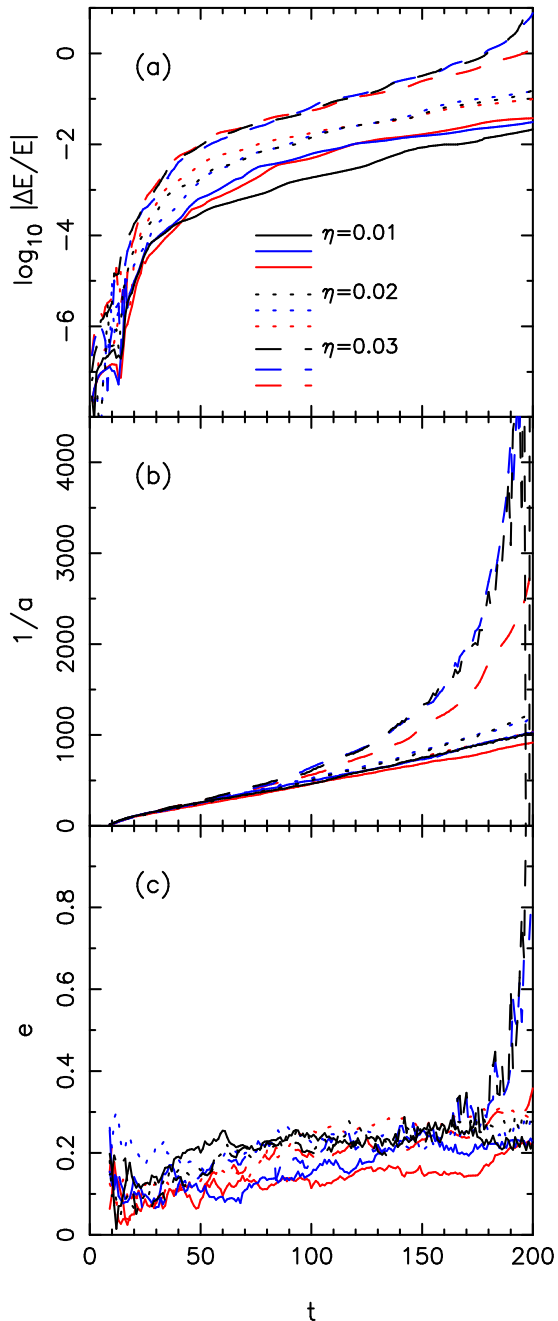


Fig. 1.— Dependence of the global energy conservation (a), binary semi-major axis (b), and binary eccentricity (c) on the N -body parameters η and ϵ , for integrations with $M_1 = M_2 = 0.02$ and $N = 0.05 \times 10^6$. *Black lines:* $\epsilon = 1 \times 10^{-5}$; *blue lines:* $\epsilon = 5 \times 10^{-5}$; *red lines:* $\epsilon = 1 \times 10^{-4}$.

major axis obeys $a(t)^{-1} \approx C_1(N) + C_2(N)t$, i.e. the binary’s binding energy increases almost linearly with time, and the hardening rate is a monotonically decreasing function of N . An approximately linear dependence of $1/a$ on time is characteristic of both the “full loss cone” (small N) and “empty loss cone” (large N) regimes (Paper I). If the loss cone were completely full, however, the hardening rate would be independent of N , clearly a poor description of Figure 2.

We define the instantaneous hardening rate to be

$$s(t) \equiv \frac{d}{dt} \left(\frac{1}{a} \right). \quad (6)$$

Figure 3 shows $s(t)$ for each of the integrations, computed by fitting smoothing splines to $a^{-1}(t)$ and differentiating. The constancy of s at late times ($t \gtrsim 150$) is apparent; aside from some wiggles, the dependence of $1/a$ on time is well approximated as a linear function. To a good approximation, we can therefore identify a *unique*, late-time hardening rate $\bar{s}(N, M)$ with each of the integrations. We computed \bar{s} by fitting a straight line to $a^{-1}(t)$ in the time intervals $150 \leq t \leq 250$. Figure 4 shows the results, plotted versus particle number N . The N -dependence of the mean hardening rate is approximately

$$\begin{aligned} \log_{10} \bar{s} &\approx 4.5 - 0.81 \log_{10} N, \quad M_1 = M_2 = 0.02, \\ &\approx 2.7 - 0.33 \log_{10} N, \quad M_1 = M_2 = 0.00. \end{aligned}$$

or

$$\begin{aligned} \frac{d}{dt} \left(\frac{1}{a} \right) &\approx 3.3 \times 10^4 N^{-0.81}, \quad M_1 = M_2 = 0.02, \\ &\approx 5.0 \times 10^2 N^{-0.33}, \quad M_1 = M_2 = 0.005. \end{aligned}$$

The very nearly linear increase of the binary’s binding energy with time seen in all these simulations was something of a surprise. While $a^{-1}(t)$ is predicted to be *approximately* linear in both the full- and empty-loss-cone regimes, at least at times before the binary has removed much mass from the core (Paper I), the theory on which this prediction is based is only approximate. It will be interesting to see if the constant rate of hardening observed here is a very general feature of binary evolution.

Also of interest is the evolution of the binary’s eccentricity (Figure 5). The two massive particles

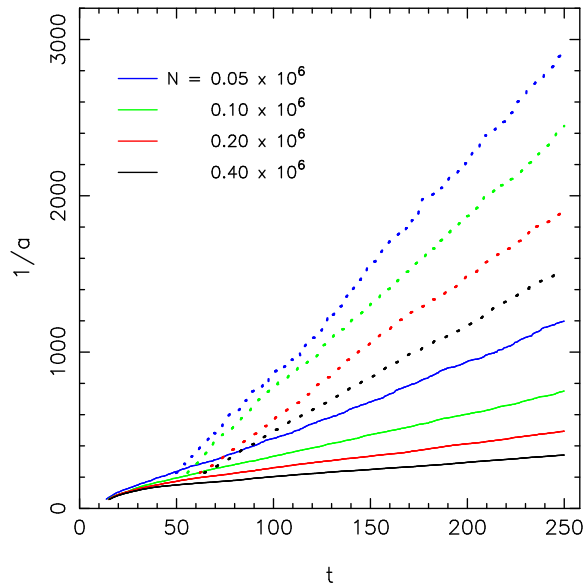


Fig. 2.— Evolution of binary semi-major axis. *Solid lines:* $M_1 = M_2 = 0.02$; *dotted lines:* $M_1 = M_2 = 0.005$.

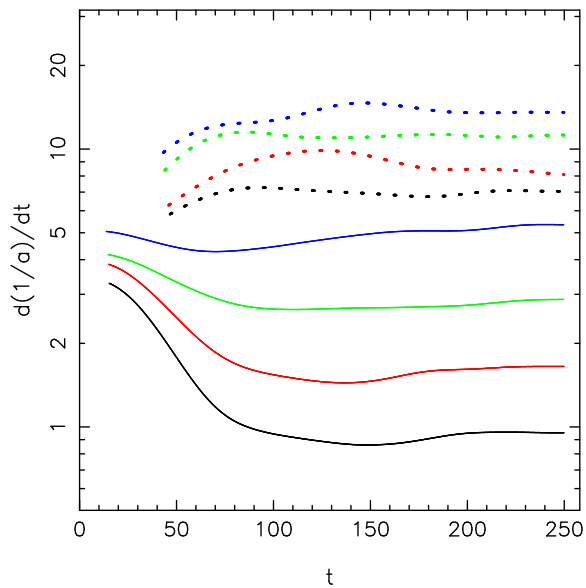


Fig. 3.— Evolution of binary hardening rate. Color scheme is the same as in Figure 2. *Solid lines:* $M_1 = M_2 = 0.02$; *dotted lines:* $M_1 = M_2 = 0.005$.

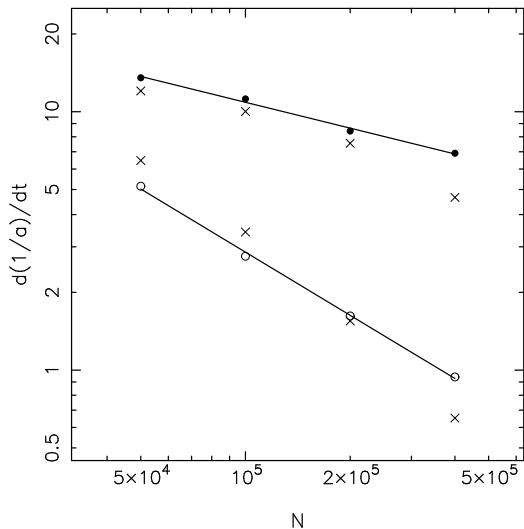


Fig. 4.— Mean binary hardening rates in the interval $150 \leq t \leq 250$ as a function of N . *Open circles*: $M_1 = M_2 = 0.02$; *filled circles*: $M_1 = M_2 = 0.005$. The lines are least-squares fit to the N -body hardening rates. Crosses show the predictions from loss-cone theory, as discussed in the text.

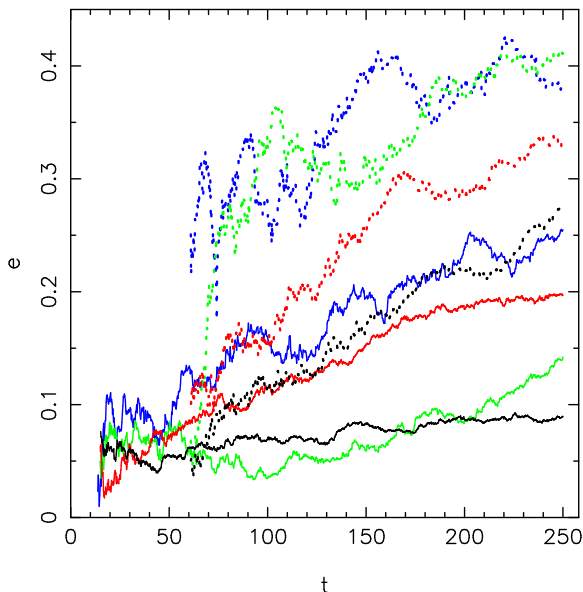


Fig. 5.— Evolution of binary eccentricity. Color scheme is the same as in Figure 2. *Solid lines*: $M_1 = M_2 = 0.02$; *dotted lines*: $M_1 = M_2 = 0.005$.

are introduced into the galaxy model on approximately circular orbits with respect to the galaxy center, but encounters with stars induce a non-zero eccentricity even before the time that the separation has fallen to a_h , and the eccentricity continues to evolve as the binary ejects stars. There is an N -dependence here as well, in the sense that e tends to evolve less with increasing N , although the trend is obscured by noise. In addition, for larger N , the “initial” eccentricity (i.e. the value of e when the binary first becomes hard) tends to be smaller, due presumably to the smaller size of random perturbations from passing stars. Figure 5 suggests that the eccentricity evolution of a binary in a real galaxy with much larger N would be very small, although larger particle numbers will be required to verify this conclusion.

The center of mass of the binary wanders quasi-randomly due to encounters with stars, both distant, elastic encounters (Chatterjee et al. 2002; Laun & Merritt 2004) and “super-elastic” encounters in which the binary’s binding energy is transformed into linear momentum during ejections (Merritt 2001). Figure 6 shows this gravitational Brownian motion in the four integrations with largest N . These plots show the motion of the binary with respect to a fixed (inertial) frame; because the N -body model as a whole drifts in space, there is also a systematic drift of the binary’s mean position. We attempted to “take out” this drift by computing the position of the binary with respect to the galaxy’s density center at each time step. However the structure of the galaxy models, with their large, constant-density cores, made this difficult since the position of the estimated density center tended to vary from time step to time step with an amplitude almost as great as that of the Brownian motion. In any case, one can estimate the amplitude of the “random” component of the motion from Figure 6, and it is quite similar to what has been found in other N -body simulations with similar initial conditions (Chatterjee et al. 2003; Makino & Funato 2004), as well as with the expectations from encounter theory (Merritt 2004). Below we address the question of whether the binary’s Brownian motion might influence its hardening rate.

The presence of the binary affects the central properties of the galaxy, although only slightly. Figure 7 shows the evolution of the central density

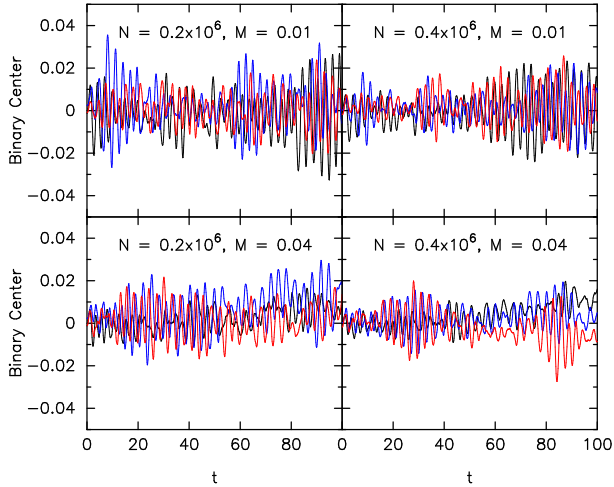


Fig. 6.— Motion of the binary center of mass in the four integrations with largest N . The position of the binary is measured with respect to the fixed (inertial) frame; the systematic change that is apparent in some of the plots is due to an overall drift of the N -body model. *Black lines: x_{CM} ; blue lines: y_{CM} ; red lines: z_{CM} .*

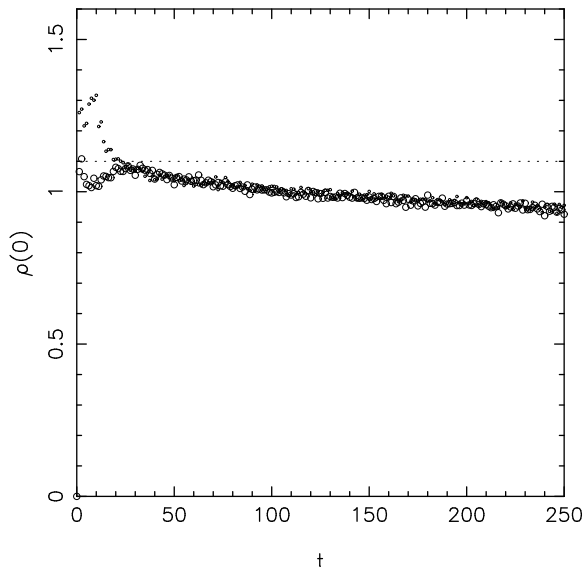


Fig. 7.— Evolution of the central density of the galaxy, defined as the mean density within a sphere of radius 0.2 centered on the binary, in the two integrations with $N = 0.4 \times 10^6$. *Small dots: $M_1 = M_2 = 0.02$; open circles: $M_1 = M_2 = 0.005$.* Dashed line shows the mean density within $r = 0.2$ in the initial model.

in the two integrations with $N = 0.4 \times 10^6$; here the density was defined as the mass in a sphere of radius 0.2 centered on the binary divided by the volume of the sphere. The introduction of the binary into the model at $t = 0$ causes an impulsive change in the local density, particularly in the case of the more massive binary, but the effect is transient and thereafter the density changes only by $\sim 15\%$ over the course of the integration, due presumably to ejection of stars. The evolution in central density was almost the same for these two integrations and depended only weakly on N as well. Such modest changes in the central properties of the galaxy models could hardly be responsible for the strong dependence of binary hardening rate on M and N seen in Figures 2-4.

4. A Model for Binary Evolution

In an infinite, homogeneous background with fixed properties (density, velocity dispersion etc.), the binary's hardening rate is given by

$$s \equiv \frac{d}{dt} \left(\frac{1}{a} \right) = H \frac{G\rho}{\sigma} \quad (9)$$

with ρ and σ the stellar density and 1D velocity dispersion; H is a dimensionless decay rate that depends on the binary semi-major axis, as well as on other binary parameters such as mass ratio and eccentricity. Scattering experiments give $H \approx 16$ for a hard ($a \ll a_h$), equal-mass binary (Hills 1983; Mikkola & Valtonen 1992; Quinlan 1996; Merritt 2001). If we set ρ and σ to their values in our Plummer-model galaxy at $t = 0$, equation 9 with $H = 16$ predicts $s \approx 35$, independent of M and N . By comparison, the *largest*, late-time decay rate found in these integrations (for $M = 0.01$ and $N = 0.05 \times 10^6$) was $s \approx 14$ (Figures 3, 4), not terribly different. However, the strong dependence of the decay rate on M and N in the simulations is clearly inconsistent with this simple model.

As discussed in Paper I, there is a natural explanation for the N -dependence of the hardening rate. After roughly a single galaxy crossing time, the binary has ejected all of the stars on intersecting orbits. Subsequent interactions between the binary and the stars occur at a rate that is limited by how quickly new stars can be scattered into the binary's loss cone. The latter is defined as the set of orbits with pericenters $r_p < Ka(t)$,

with K a number of order unity; this expression reflects the expectation that stars will be ejected from the binary whenever they pass a distance $\sim a$ from its center of mass. But the scattering of stars onto low-angular-momentum orbits depends on the two-body relaxation time, hence on the mean stellar mass, hence on N , and so one expects the hardening rate of the binary to be N -dependent as well.

As a first step toward testing this model, we asked whether star-star encounters might be so frequent in the N -body models that the binary’s loss cone is maintained in a continuously populated state. The standard measure of the loss-cone refilling rate in a spherical, steady-state galaxy is $q(E)$, defined as

$$q(E) \equiv \frac{(\delta J)^2}{J_{lc}^2}. \quad (10)$$

(Lightman & Shapiro 1977). Here δJ is the change over one radial period in the angular momentum of a star on a low- J orbit, and J_{lc} is the angular momentum of an orbit at the edge of the loss cone. A value $q(E) \gg 1$ implies that the loss cone orbits at energy E are re-populated at a much higher rate than they are de-populated by the central sink (in this case, the binary black hole), and the loss cone remains nearly full. A value $q \ll 1$ implies that the loss cone is essentially empty, and repopulation must take place diffusively, as stars scatter in from $J \gtrsim J_{lc}$.

We computed $q(E)$ in our Plummer-model galaxies, ignoring any effect of the binary on the galaxy. We used the precise, orbit-averaged definition of $q(E)$ given by equation (8) in Paper I. The results are shown in Figure 8. The binary parameters appear implicitly in q , since $J_{lc}^2 = 2GM r_t$ with $r_t = Ka$ the radius of the capture sphere. Figure 8 shows q as a function of E for the eight different combinations of (N, M) in our N -body integrations. We considered two values for J_{lc} , $J_{lc}^2 = 2GM a_h$ and $J_{lc}^2 = 2GM a_h/10$; the first value is the approximate “size” of the loss cone when the hard binary first forms, and the latter value is appropriate when a has decreased by a factor of 10, roughly the maximum amount of decay seen in these integrations (Fig. 2). Figure 8 suggests that the integrations with the higher-mass binary, $M = 0.04$, took place mostly in the “empty loss cone” regime, $q \lesssim 1$, while the inte-

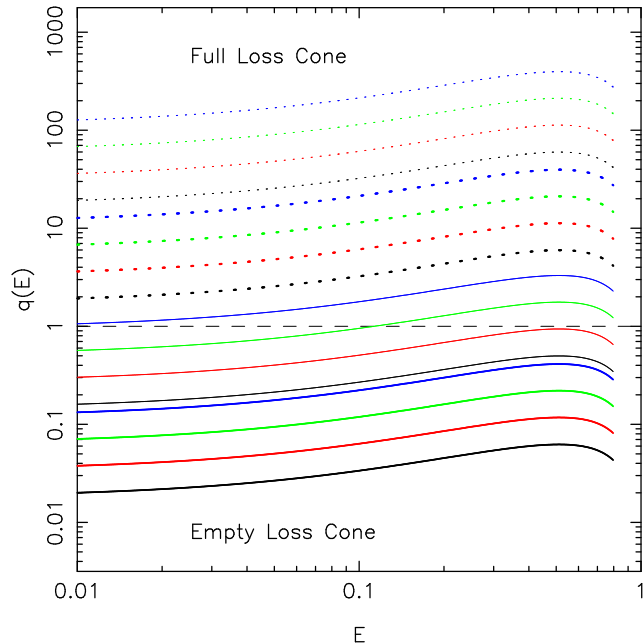


Fig. 8.— The quantity $q(E)$ that measures the degree to which the binary’s loss cone is repopulated by encounters. Color scheme is the same as in Fig. 2. *Solid lines*: $M_1 = M_2 = 0.02$; *dotted lines*: $M_1 = M_2 = 0.005$. The thicker curves in each group are for $r_t = a_h$, the approximate radius of the loss sphere when the binary first forms, and the thinner curves are for $r_t = a_h/10$, corresponding to an evolved binary. These curves suggest that the evolution of the more massive binary in our N -body integrations took place mostly in the “empty loss cone” regime, while the evolution of the less massive binary took place mostly in the “full loss cone” regime.

grations with $M = 0.01$ were mostly in the “full loss cone” regime, $q \gtrsim 1$.

This result provides a natural explanation for the different N -dependence of the decay rates in the two sets of integrations. When the loss cone is empty, $q \ll 1$, re-population takes place diffusively, as stars are scattered by other stars onto low-angular-momentum orbits. The scattering rate scales inversely with the relaxation time, or as $\sim 1/N$. Indeed, the binary decay rate for $M = 0.04$ scales almost as N^{-1} (Fig. 4). On the other hand, when the loss cone is full, $q \gg 1$, the decay rate is nearly independent of the relaxation time, since (by assumption) scattering occurs so quickly that orbits are never depleted. The much weaker dependence of s on N for $M = 0.01$ (Fig. 4) is qualitatively consistent with this prediction.

We tested this model more carefully, by computing the expected hardening rate of the binary, under the assumption that the supply of stars was limited by the rate of loss cone repopulation. The flux of stars into the binary’s loss cone (mass per unit time) in a steady-state spherical galaxy is given approximately by

$$\mathcal{F}(E)dE \approx 4\pi^2 J_{lc}^2(E)q(E) \frac{f(E)}{\ln R_0^{-1}} dE \quad (11)$$

(Paper I), where $f(E)$ is the phase-space mass density of stars at energy E , and $R_0(E)$ is the effective, dimensionless size of the loss cone as seen by a star of energy E ; an approximate expression for $R_0(E)$ is given by Cohn & Kulsrud (1978). If all of the stars scattered into the loss cone are assumed to interact instantaneously with the binary, its decay rate is roughly

$$s \equiv \frac{d}{dt} \left(\frac{1}{a} \right) \approx \frac{2\langle C \rangle}{aM} \int \mathcal{F}(E)dE \quad (12)$$

where $\langle C \rangle$ is the average value of the dimensionless energy change during a single star-binary encounter, $C \equiv (M/2m_*) (\Delta E/E)$ (Hills 1983). In the limit $a \ll a_h$, $\langle C \rangle$ is constant and roughly equal to one. While equation (12) with constant $\langle C \rangle$ is unlikely to give a good description of the early evolution of the binary, when $a \lesssim a_h$, it should reproduce the late-time hardening rate of the binary fairly well. Figure 4 shows that this is indeed the case; we set $r_t = a$ and $\langle C \rangle = 1.25$, and evaluated s from equation (12) at the final

value of a reached in each integration. Given the simplicity of the model, the agreement with the N -body hardening rates is remarkably good. Deviations between theory and simulation appear to be greatest at largest N ; this may be due to the fact that the binary separation does not fall far below a_h in these integrations.

We conclude that the binary hardening rates observed in the N -body simulations – including their dependence on M and N – are consistent with the predictions of loss cone repopulation theory. In particular, the integrations with $M = 0.04$ exhibit the $\sim N^{-1}$ scaling of hardening rate with particle number that is characteristic of an “empty,” diffusively-repopulated loss cone.

Brownian motion of the binary might also affect its decay rate, by enhancing the diffusion of stars into the binary’s loss cone. In Paper I, a simple model was presented for this process. Equation (85) from that paper gives the diffusion time (i.e. the time for the binary’s loss cone to be repopulated) due to Brownian motion as

$$t_{Brown} \approx \frac{(Ka)(2E)^{7/2}}{6\pi G^2(M_1 + M_2)^2 \mathcal{A}^2}. \quad (13)$$

Here Ka is defined as above, as the distance from the binary’s center within which the gravitational slingshot is effective; E is the orbital energy, assuming a Keplerian potential around the black hole (the potential from the other stars was ignored in this model); and \mathcal{A}^2 is the mean square acceleration experienced by the binary due to gravitational perturbations from stars. Adopting equation (76) from Paper I for \mathcal{A} , and setting $E = \sigma^2$, the orbital energy of a star near the binary’s gravitational influence radius, we find in N -body units

$$t_{Brown} \approx 10^2 N_6 M_{-2} a_{-2} \quad (14)$$

where $N_6 \equiv N/10^6$, $M_{-2} \equiv (M_1 + M_2)/0.01$, and $a_{-2} \equiv a/0.01$.

This time scale should be compared with the time scale for stars to diffuse into the binary’s loss cone due to star-star encounters, or $t_{diff} \approx P(E)/q(E)$ with $P(E)$ the orbital period. Evaluating q and P at the binary’s gravitational influence radius, $E \approx E_h = \sigma^2$, we find

$$t_{diff} \approx \{0.59, 0.15\} q(E_h)^{-1} \quad (15)$$

for $M = \{0.04, 0.01\}$. In the simulations with the smaller binary, Figure 8 shows that q is always greater than ~ 1 , implying $t_{diff} \lesssim 0.15$. This is much shorter than t_{Brown} for any (N, a) considered here, from which it follows that Brownian motion had almost no effect on loss-cone repopulation. In effect, the smaller binary’s loss cone was maintained in such a full state by star-star encounters that the additional influence of the binary’s motion was negligible. In the case of the more massive binary, we have

$$\frac{t_{diff}}{t_{Brown}} \approx (10^3 q N_6 a_{-2})^{-1}. \quad (16)$$

Figures 2 and 8 suggest that this ratio might have approached unity at late times in the simulations with smallest N , but generally was much smaller than one, again suggesting that the influence of Brownian motion on the binary’s evolution was small.

5. Comparison with Other Work

Our initial conditions were chosen to be identical with those of Chatterjee, Hernquist & Loeb (2003) (CHL), who used a rather different N -body algorithm to follow the evolution of massive binaries at the centers of Plummer-model galaxies. These authors present detailed results for only two integrations, with $M_1 = M_2 = 0.00125$ and $M_1 = M_2 = 0.02$; the latter values match our more massive binary, and Figure 2 in CHL shows the evolution of $1/a$, e and $\rho(0)$ for an integration with $N = 0.2 \times 10^6$. The evolution found by CHL for e and $\rho(0)$ appears consistent with what we find here for the same values of M and N . However our results for the binary hardening rate differ from theirs, in two respects. (1) CHL observed binary hardening rates $s = (d/dt)(1/a)$ that were significantly time-dependent, with $1/a$ sometimes increasing as weakly as $\sim t^{0.5}$, rather than the linear dependence observed here. For instance, their Fig. 2 shows a gradually falling decay rate in the case ($M_1 = M_2 = 0.02$, $N = 0.2 \times 10^6$), with a value of $1/a$ at $t = 250$ of ~ 360 , compared with our value of ~ 500 . (2) While CHL also found that hardening rates tended to fall with increasing N , they state that “ s falls systematically until there are roughly 200,000 – 400,000 stars, when it stabilizes to a particular value, s_0 .” Unfortunately, CHL provided no plots of $s(t)$ or $s(N)$ against

which this result could be verified; however they did quote some particular values for s_0 , e.g. $s_0 \approx 8$ when $M_1 = M_2 = 0.005$. This is consistent with the value of s that we measure for large N in our integrations with the same binary mass (Fig. 4), but we observe no tendency for the hardening rate to “stabilize” at large N , either for this binary or for the more massive one that we integrated.

CHL compared the results of their integrations with the predictions of *local* theory, via an equation similar to our equation (9). Since that equation predicts no dependence of hardening rates on M or N , CHL invoked the mass dependence of the binary’s Brownian motion to explain their results. CHL suggested (without presenting a quantitative theory) that the larger wandering radius in integrations with smaller M and N would translate into larger rates of interaction between the binary and the stars. The “stabilization” of the hardening rate which they observed at large N (and which we do not observe) was attributed to a kind of Brownian-motion-mediated feedback process, in which the binary maintains a constant supply rate by modulating the local density of stars. However no supporting evidence for this model was presented; for instance, it was not demonstrated that the central density was actually regulated by the binary in their N -body integrations, or that the amplitude of the Brownian wandering increased with N in the manner postulated.

Decay of binary black holes in Plummer-model galaxies was also investigated by Hemsendorf et al. (2002) (HSS). Those authors placed two equal-mass particles, $M_1 = M_2 = 0.01$, at the center of the galaxy and carried out integrations with particle numbers $N = (0.033, 0.065, 0.131) \times 10^6$. The black hole particles were placed on initially eccentric orbits at radii ± 0.5 , farther from the center than in our or in CHL’s simulations. Furthermore the models were integrated only until $t = 60$, and in the case of the largest N , only until $t \approx 40$. Comparison with our Figure 3 suggests that the hardening rate of the binary at $t \approx 60$ might be rather different from its late-time value. HSS found a mean hardening rate for all of their integrations of $s \approx 6 - 7$ (their Fig. 3), quite consistent with the early hardening rates found here (Fig. 3), especially if one takes into account that their binary mass lies midway between our two. HSS observed only a slight dependence of decay

rate on N , but this too is consistent with what we find at early times (Fig. 3). HSS observed a much stronger evolution of the binary’s eccentricity, but this may be due to their large *initial* eccentricity, $e \approx 0.8 - 0.9$. Eccentric binaries are expected to evolve in the direction of increasing eccentricity (Mikkola & Valtonen 1992; Quinlan 1996).

A number of other N -body studies of binary evolution have been carried out using galaxy models with large cores (Ebisuzaki et al. 1991; Makino et al. 1993; Governato et al. 1994), though most of these used too few particles to show a dependence of hardening rate on N . One exception was the recent study by Funato & Makino (2003), who considered binaries in King (1966)-model galaxies with particle numbers as high as 1.0×10^6 . These authors also failed to reproduce the stabilization of the binary hardening rate at large N found by CHL.

6. Implications for Binary Evolution in Real Galaxies

The strong N -dependence of the binary hardening rate in our simulations makes it dangerous to extrapolate our results to real galaxies. Such an extrapolation may nevertheless be justified in the case of our more massive binary, which appeared (Fig. 8) to be in the “empty loss cone” regime. Massive binaries in real galaxies are also expected to be in this regime (Paper I), at least in the absence of any additional mechanisms for loss-cone repopulation, and the N -dependence of the hardening rate observed here for the more massive binary might therefore be valid for much larger N .

We begin by noting that the degree of evolution, as measured by the ratio $a_h/a(t_f)$ between initial and final binary separations, was equal to $\sim (21, 14, 8.8, 6.2)$ for $N = (0.05, 0.1, 0.2, 0.4) \times 10^6$ in the simulations with the more massive binary. If the binary’s actual mass was $10^8 M_\odot$, the $M - \sigma$ relation (Ferrarese & Ford 2005) implies a galaxy velocity dispersion of $\sigma \approx 180 \text{ km s}^{-1}$, so $a_h \approx 1.7 \text{ pc}$ and the final scaled separations become $(0.025, 0.12, 0.19, 0.27) \text{ pc}$. Coalescence of an equal-mass binary in a Hubble time due to gravitational wave emission requires $a_h/a \gtrsim 20$ (Merritt & Milosavljevic 2004), so the integration with smallest N can be said to have just reached the gravitational radiation regime.

But the implied degree of hardening in a real galaxy is much less than this if we take into account the likely scaling of the hardening rate with N . Ignoring possible changes in the central density of the host galaxy (such changes were small in the integrations reported here), equation (9a) implies

$$\begin{aligned} T_{decay} &\equiv \left[a \frac{d}{dt} \left(\frac{1}{a} \right) \right]^{-1} & (17a) \\ &\approx 2.0 \times 10^4 [G\rho(0)]^{-1/2} \left(\frac{r_0}{a} \right) N^{0.17b} \end{aligned}$$

or

$$\frac{T_{decay}}{T_{cr}} \approx 2 \times 10^7 \left(\frac{r_0/a}{10^3} \right) \left(\frac{N}{10^{11}} \right)^{0.81} \quad (18)$$

with $T_{cr} \equiv (G\rho(0))^{-1/2}$ the galaxy crossing time. Equation (18) suggests that binary hardening times in real galaxies would be very long, of order 10^7 crossing times and much greater than the age of the universe. In effect, the binary would “stall.”

A very different conclusion was reached by Chatterjee et al. (2003), who *assumed* that the binary hardening rates observed by them at $N \approx 0.2 - 0.4 \times 10^6$ would remain constant even for much larger values of N .

Of course our prediction is based on a rather unphysical (too homogeneous) galaxy model, an unrealistic (too large) choice for the mass of the binary, and unlikely initial conditions (with the two black holes deposited symmetrically about the center of the galaxy, rather than arriving there as a result of a galactic merger). Binary hardening rates in galaxies with steeply-rising central densities might be significantly larger than implied by equation (18). Upcoming papers in this series will attempt to correct these deficiencies with more realistic galaxy models and more physically-motivated initial conditions.

7. Conclusions

The evolution of a massive binary at the center of a galaxy with a large, constant-density core was followed using a high-accuracy N -body code and a special-purpose computer cluster. Two values for the binary mass were considered: $(M_1 + M_2)/M_{gal} = (0.04, 0.01)$. The binary’s hardening rate exhibited a clear N -dependence, consistent

with the predictions of collisional loss-cone repopulation theory. In the simulations with $M_1 + M_2 = 0.04M_{gal}$ and large particle number, $N \gtrsim 0.2 \times 10^6$, the binary appeared to be nearly in the “empty loss cone” regime believed to characterize real galaxies (in the absence of other mechanisms for loss-cone refilling): the hardening rate decreased almost as steeply as N^{-1} . We observed no indication that the binary hardening rate “stabilizes” at particle numbers greater than $N \approx 0.2 \times 10^6$, or that the binary’s evolution is strongly affected by its Brownian motion, as claimed in a recent study based on a more approximate N -body treatment (Chatterjee, Hernquist & Loeb 2003).

Our results demonstrate the feasibility of N -body simulations of binary black hole evolution that mimic the behavior expected in systems of much larger N . Even larger particle numbers, $N \gtrsim 10^6$, will be required to correctly reproduce the evolution of binary black holes in more realistic galaxy models with higher central densities and less massive binaries. Direct-summation N -body simulations with such high particle numbers are now becoming feasible with the advent of parallel, special-purpose computers like gravitySimulator. Future papers in this series will present the results of such simulations.

DM acknowledges support from grants AST-0206031, AST-0420920 and AST-0437519 from the NSF, grant NNG04GJ48G from NASA, and grant HST-AR-09519.01-A from STScI. PB and RS acknowledge support from grant SFB-439 from the Deutsche Forschungsgemeinschaft. This work was supported in part by the Center for Advancing the Study of Cyberinfrastructure at the Rochester Institute of Technology.

REFERENCES

- Aarseth, S. J. 1999, *PASP*, 111, 1333
- Aarseth, S. J. 2003, *Ap&SS*, 285, 367
- Baranov, A. S. 1984, *Soviet Astronomy*, 28, 642
- Chatterjee, P., Hernquist, L., & Loeb, A. 2002, *ApJ*, 572, 371
- Chatterjee, P., Hernquist, L., & Loeb, A. 2003, *ApJ*, 592, 32
- Cohn, H., & Kulsrud, R. M. 1978, *ApJ*, 226, 1087
- Ebisuzaki, T., Makino, J., & Okumura, S. K. 1991, *Nature*, 354, 212
- Ferrarese, L., & Ford, H. 2005, *Space Science Reviews*, 116, 523
- Fukushige, T., Makino, J., & Kawai, A. 2005, *ArXiv Astrophysics e-prints*, arXiv:astro-ph/0504407
- Governato, F., Colpi, M., & Maraschi, L. 1994, *MNRAS*, 271, 317
- Harfst, S. et al. 2005, in preparation
- Heggie, D. C., & Mathieu, R. D. 1986, *LNP Vol. 267: The Use of Supercomputers in Stellar Dynamics*, 267, 233
- Hemsendorf, M., Sigurdsson, S., & Spurzem, R. 2002, *ApJ*, 581, 1256
- Hills, J. G. 1983, *AJ*, 88, 1269
- Kandrup, H. E., Sideris, I. V., Terzić, B., & Bohn, C. L. 2003, *ApJ*, 597, 111
- King, I. R. 1966, *AJ*, 71, 64
- Laun, F., & Merritt, D. 2004, *ArXiv Astrophysics e-prints*, arXiv:astro-ph/0408029
- Lightman, A. P., & Shapiro, S. L. 1977, *ApJ*, 211, 244
- Makino, J., & Aarseth, S. J. 1992, *PASJ*, 44, 141
- Makino, J., & Funato, Y. 2004, *ApJ*, 602, 93
- Makino, J., Fukushige, T., Okumura, S. K., & Ebisuzaki, T. 1993, *PASJ*, 45, 303
- Merritt, D. 2001, *ApJ*, 556, 245
- Merritt, D. 2004, *ArXiv Astrophysics e-prints*, arXiv:astro-ph/0405351
- Merritt, D., & Milosavljevic, M. 2004, *ArXiv Astrophysics e-prints*, arXiv:astro-ph/041036
- Merritt, D., & Poon, M. Y. 2004, *ApJ*, 606,
- Mikkola, S., & Valtonen, M. J. 1992, *MNRAS*, 259, 115
- Milosavljević, M., & Merritt, D. 2001, *ApJ*, 563, 34

- Milosavljević, M., & Merritt, D. 2003, *ApJ*, 596, 860 (Paper I)
- Plummer, H. C. 1911, *MNRAS*, 71, 460
- Quinlan, G. D. 1996, *New Astronomy*, 1, 35
- Rajagopal, M., & Romani, R. W. 1995, *ApJ*, 446, 543
- Saslaw, W. C., Valtonen, M. J., & Aarseth, S. J. 1974, *ApJ*, 190, 253
- Szell, A., Merritt, D., & Mikkola, S. 2005, *ArXiv Astrophysics e-prints*, arXiv:astro-ph/0502198
- Thorne, K. S., & Braginskii, V. B. 1976, *ApJ*, 204, L1
- Merritt, D., & Wang, J. 2005, *ApJ*, 621, L101
- Yu, Q. 2002, *MNRAS*, 331, 935
- Zier, C., & Biermann, P. L. 2001, *A&A*, 377, 23